

Pedestrian Path Prediction for Autonomous Driving at Un-Signalized Crosswalk Using W/CDM and MSFM

Xi Zhang^{ID}, Senior Member, IEEE, Hao Chen^{ID}, Wenyan Yang, Wenqiang Jin^{ID}, and Wangwang Zhu

Abstract—Pedestrian trajectory prediction is essential for collision avoidance in autonomous driving, which can help autonomous vehicles have a better understanding of traffic environment and perform tasks such as risk assessment in advance. In this paper, pedestrian path prediction at a time horizon of 2s for autonomous driving is systematically investigated using waiting/crossing decision model (W/CDM) and modified social force model (MSFM), and the possible conflict between pedestrians and straight-going vehicles at an un-signalized crosswalk is focused on. First of all, a W/CDM is efficiently developed to judge pedestrians' waiting/crossing intentions when a straight-going vehicle is approaching. Then the humanoid micro-dynamic MSFM of pedestrians who have been judged to cross is characterized by taking into account the evasion with conflicting pedestrians, the collision avoidance with straight-going vehicles, and the reaction to crosswalk boundary. The influence of pedestrian heterogeneous characteristics is considered for the first time. Moreover, aerial video data of pedestrians and vehicles at an un-signalized crosswalk is collected and analyzed for model calibration. Maximum likelihood estimation (MLE) is proposed to calibrate the non-measurable parameters of the proposed models. Finally, the model validation is conducted with two cases by comparing with the existing methods. The result reveals that the integrated method (W/CDM-MSFM) outperforms the existing methods and accurately predicts the path of pedestrians, which can give us great confidence to use the current method to predict the path of pedestrian for autonomous driving with significant accuracy and highly improve pedestrian safety.

Index Terms—Pedestrian path prediction, autonomous driving, waiting/crossing decision model (W/CDM), modified social force model (MSFM), maximum likelihood estimation (MLE), un-signalized crosswalk.

I. INTRODUCTION

NOWADAYS, progress in autonomous driving and advanced driver assistance systems (ADAS) seems to suggest that intelligent vehicles will be able to drive without human drivers soon. Currently, research studies on autonomous driving are mainly focused on the safety aspects of reducing accidents.

Manuscript received April 25, 2019; revised August 28, 2019, October 16, 2019, and December 25, 2019; accepted February 24, 2020. Date of publication March 13, 2020; date of current version May 3, 2021. This work was supported in part by the National Natural Science Foundation of China under Grant 51677118, and in part by the National Key Research and Development Plan Key Special Project under Grant 2017YFE0102000. The Associate Editor for this article was S. Arhin. (Corresponding author: Xi Zhang.)

The authors are with the School of Mechanical Engineering, Shanghai Jiao Tong University, Shanghai 200240, China, and also with the MoE Key Laboratory of Artificial Intelligence, Shanghai Jiao Tong University, Shanghai 200240, China (e-mail: braver1980@sjtu.edu.cn; hchen1989@sjtu.edu.cn; yangwenyan@sjtu.edu.cn; jinwenqiang@sjtu.edu.cn; zhuwangwang@sjtu.edu.cn).

Digital Object Identifier 10.1109/TITS.2020.2979231

In the autonomous driving domain, one of the most important challenges is the understanding of the traffic situations. Pedestrians, particularly, as a major challenge, have high dynamic range behaviors, they can frequently transform their moving direction and moving velocity in a second which always make surrounding vehicles stop or brake. Moreover, pedestrians are the most vulnerable road users and most accidents happen while they are crossing an un-signalized crosswalk [1]. Research indicates that a successful prediction of 30cm in the path of pedestrian can make the difference for collision avoidance between pedestrians and vehicles [2], [3]. Accident analysis demonstrated that emergency braking for 0.16s earlier could cut the severity of accident injuries down to 50% [4]–[6]. Thus, in order to reduce traffic accidents and protect pedestrian safety, as well as improve traffic efficiency in the context of autonomous driving, it is important to predict the possible path of pedestrians for autonomous vehicles.

So far, several pedestrian path prediction methods have been proposed, such as Extended Kalman filter [7], Neural Networks [8], [9], Social Force Model (SFM) [10], [11] and so on. Among the methods mentioned above, SFM has the advantages in predicting pedestrian path with traffic states in real time, for it can take the interaction between pedestrian and pedestrian or pedestrian and autonomous vehicle into consideration. Besides, it can obtain better prediction accuracy in the case of the limited training data, and the time consumption is significantly lower than those of the Neural Networks methods.

In this paper, in order to protect pedestrian safety and improve traffic efficiency for autonomous driving, pedestrian path prediction with straight-going vehicles at an un-signalized crosswalk is concentrated on. Aiming at this issue, W/CDM and MSFM based on the real path data are proposed. Fig. 1 shows the framework of the pedestrian path prediction process. The main contributions of this paper are summarized as follows:

1) Two efficient waiting/crossing decision models (W/CDM) are developed to judge pedestrians' waiting/crossing intentions when a straight-going vehicle is approaching based on pedestrian heterogeneous characteristics (age and gender) and traffic states.

2) Integrating sociology and social psychology, a humanoid micro-dynamic model (MSFM) is developed to predict pedestrian path which takes the evasion with conflicting pedestrians, the collision avoidance with straight-going vehicles, and the reaction to crosswalk boundary into account. In addition,

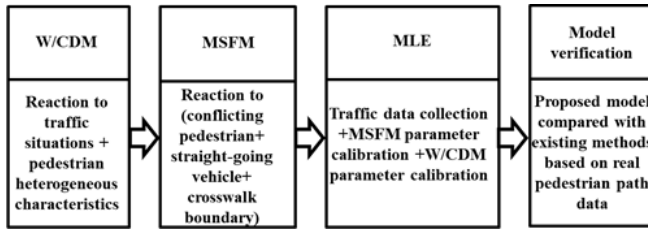


Fig. 1. Framework of the pedestrian path prediction process.

the influence of pedestrian heterogeneous characteristics (age and gender) is considered in MSFM for the first time.

3) The desired speed and relaxation time for pedestrians by age and gender type are quantified and described. To calibrate the non-measurable parameters for MSFM and W/CDM, an approximate method is proposed, namely, Maximum likelihood estimation (MLE).

4) The model validation compared with the existing methods based on real path data in two typical cases is conducted, and the results demonstrate the outperformance of the proposed method (W/CDM-MSFM) with significant accuracy.

In this paper, the reason why 2s is chosen as pedestrian path prediction horizon time is that: firstly, the pedestrian path prediction horizon time (e.g., 3s) is not suitable to be longer which will make the proposed method less sensitive to complex traffic states and less accurate. At the same time, the longer the pedestrian path prediction horizon time is, the more tedious training time and larger computing resources is. Secondly, the pedestrian path prediction horizon time (e.g., 1.5s) is meaningless to be shorter. While there is a risk of collision with pedestrians, the shorter the pedestrian path prediction horizon time is, the shorter time left for intelligent decision-making and control of autonomous vehicles is. Hence, to combine the above two reasons which are based on accuracy, efficiency and real-time considerations, the pedestrian path prediction horizon time is chosen as 2s to ensure prediction accuracy and pedestrian safety.

The rest of the paper is presented as follows. In Section II, a brief review of the related work is presented. In Section III, W/CDM based on logistic regression model is discussed. To distinguish the two models, W/CDM for pedestrian on wayside is represented by W/CDMO, W/CDM for pedestrian in crosswalk is represented by W/CDMI, and W/CDM is used as an umbrella term. In Section IV, pedestrian path prediction based on MSFM is presented. In Section V, traffic data is collected at an un-signalized crosswalk. The measurable parameters estimated from the observed path data directly are discussed, and the non-measurable parameter calibration of MSFM and W/CDM based on the MLE is conducted. In Section VI, the predicted results are compared with the existing method based on the real pedestrian path data to verify the effectiveness of the integrated method (W/CDM-MSFM). In Section VII, the conclusions of this paper are given.

II. RELATED WORK

In the past few years, there are several existing researches related to pedestrian path prediction. Schneider and Gavrila [12] considered Extended Kalman Filters (EKF)

based on single dynamical models combining several such basic models (CV, CA) for pedestrian path prediction at short time horizons. Raul *et al.* [13] proposed a balanced Gaussian process dynamical model (B-GPDM) to predict future pedestrian paths, poses, and intentions up to 1s in advance. Li *et al.* [14] presented an efficient approach for pedestrian path prediction in densely crowded environments. An auto-encoder feature learning model and a Gaussian process regression prediction model were considered in the proposed approach. Keller and Gavrila [15] presented a study on action classification and pedestrian path prediction at short sub-second time intervals. Saleh *et al.* [16] proposed a radical end-to-end data-driven approach for long-term intent prediction of pedestrians' trajectories based on Long Short-Term Memory (LSTM) network. The results showed that the approach achieved higher accuracies with a small lateral position error of 0.48m. Yi *et al.* [17] presented a deep neural network (Behavior-CNN) to model pedestrian behaviors in crowded scenes, and walking path prediction showed the effectiveness of Behavior-CNN on pedestrian behavior modeling. These approaches, such as EKF, B-GPDM and so on, may not need a lot of training data, however, the accuracy of prediction and length of time horizon still need to be improved. Other Neural Networks approaches achieved better performance for pedestrian path prediction, but on the other side, the successes of these deep learning methods were at the expense of massive data, tedious training time and large computing resources, and may not be suitable for the real-time prediction system for autonomous vehicle.

The above methods mainly considered the path prediction for an independent pedestrian without other traffic states into consideration, which was insufficient for the interaction between pedestrian and pedestrian or pedestrian and vehicle or pedestrian and other traffic states. To mine more information, some researchers concentrated on the analyzed pedestrian behavior and dynamic simulation based on SFM with various traffic states for pedestrian path prediction. Zeng *et al.* [18] used SFM to model the pedestrian behavior at signalized crosswalks. The predicted path was compared with the observed path which demonstrated the advantage of the hybrid approach. Liu *et al.* [19] developed the pedestrian behavior model based on SFM with various interactions on pedestrian dynamics at crosswalks, and the predicted path was verified with real data extracted from video. Cao *et al.* [20] established a SFM to simulate the interactions between pedestrians and vehicles at unmarked roadways. The real trajectories showed a good agreement with the predicted trajectories which indicated the accuracy of the model. Anvari *et al.* [21] presented a three-layered microscopic mathematical model to simulate the behavior of pedestrians and vehicles in the shared space layouts. A SFM was used for the mixed traffic to produce the feasible path and simulate the shared space environment, and the predicted path was in good agreement with the real path. Rinke *et al.* [22] developed a multi-layer approach based on SFM to represent the movement of road users and their interaction, and the predicted path was compared with the observed path in different traffic situations. Huang *et al.* [23] developed a microscopic simulation model based on SFM

for cyclist behavior analysis at un-signalized intersection with heterogeneous traffic. Simulation results showed that the predicted path could represent cyclist crossing behavior as in the real world. Compared with the prediction methods only considered an independent pedestrian above, these approaches usually take the interaction of pedestrians and other traffic states into account. However, the influence of pedestrian heterogeneous characteristics which are important factors in improving the accuracy of pedestrian path prediction are not covered in these methods.

Different from the above work, this paper explores pedestrian path prediction based on W/CDM-MSFM at un-signalized crosswalk for autonomous driving. Pedestrian heterogeneous characteristics for W/CDM-MSFM based on the real traffic data are taken into account for the first time, at the same time, integrating sociology and social psychology, the collision avoidance with pedestrians and straight-going vehicles, and the reaction to crosswalk boundary are taken into account in the humanoid microscopic dynamic MSFM for improving pedestrian path prediction accuracy. In addition, a novel composite force is developed to present the pedestrian force from the conflicting straight-going vehicle. The pedestrian heterogeneous characteristics by age and gender type are quantified and analyzed, and the non-measurable parameters of the models are calibrated by the MLE. Compared with the existing methods, the proposed W/CDM-MSFM can predict pedestrian path timely, accurately and adaptively, and present the feasibility to improve pedestrian safety and traffic efficiency for autonomous driving.

III. WAITING/CROSSING DECISION MODEL FOR PEDESTRIAN PATH PREDICTION

It is supposed that all the pedestrians facing an un-signalized crosswalk choose to cross when the surrounding traffic situation is safe and wait once the situation is insecure. However, some pedestrians may react to the insecure situation with different strategies which may lead to a potential conflict with vehicles [24]. For instance, certain pedestrians may enter the crosswalk and ignore the danger of the approaching straight-going vehicle, which threatens the safety of them. Generally speaking, as the rise of the autonomous driving industry, it is important for the autonomous vehicle to recognize the pedestrians' waiting/crossing intentions before they enter the crosswalk. Inspired by the developed model in Liu *et al.* [19], a waiting/crossing decision model for pedestrians on the wayside (W/CDMO) based on binary logistic regression model is extended to estimate the probability of pedestrians' waiting/crossing decision, which is formulated as follows. In this model, in addition to considering the similar time to collision (TTC) as in Liu *et al.* [19], the heterogeneous pedestrian characteristics for age and gender type, group size and vehicle type which are important factors in improving the accuracy of predicting pedestrians' real waiting/crossing intentions are also taken into consideration.

$$P_o(\text{crossing}) = \frac{\exp(\lambda_0 + \lambda_1 X_1 + \lambda_2 X_2 + \dots + \lambda_n X_n)}{1 + \exp(\lambda_0 + \lambda_1 X_1 + \lambda_2 X_2 + \dots + \lambda_n X_n)} \quad (1)$$

where $X_1 \dots X_n$ are the independent variables of influencing factors such as age type, gender type, group size, time to

TABLE I
INDEPENDENT VARIABLES AND VARIABLE CODING

Variable coding	Individual attributes			Traffic
	Gender	Age	Group	Vehicle
1	Male	Young(18-30)	1	Car
2	Female	Middle-aged(30-55)	2-5	Medium
3	/	Old(>55)	>5	Large bus

collision (TTC), vehicle type; TTC is determined as the time to the potential collision point if the vehicle keeps the current speed and direction; $\lambda_0 \dots \lambda_n$ are model coefficients estimated by the MLE.

Meanwhile, when pedestrians have entered into the crosswalk, they may also choose a quick stopping or crossing to avoid the collision when a straight-going vehicle is approaching. Thus, it is equally important for the autonomous vehicle to recognize the pedestrians' waiting/crossing intentions after they have entered into the crosswalk. Inspired by the developed model in Liu *et al.* [19], another waiting/crossing decision model for pedestrians in the crosswalk (W/CDMI) based on binary logistic regression model is extended to represent the strategy chosen by the pedestrian, which is represented as follows. In this model, in addition to considering the same time difference as in Liu *et al.* [19], the heterogeneous pedestrian characteristics for age and gender type, group size and vehicle type are also taken into account.

$$P_l(\text{crossing}) = \frac{\exp(\mu_0 + \mu_1 Y_1 + \mu_2 Y_2 + \dots + \mu_n Y_n)}{1 + \exp(\mu_0 + \mu_1 Y_1 + \mu_2 Y_2 + \dots + \mu_n Y_n)} \quad (2)$$

where $Y_1 \dots Y_n$ are the independent variables of influencing factors such as age type, gender type, group size, time difference (TD) and vehicle type; TD is determined as the vehicle arrival time to the potential collision point minuses that of pedestrian; $\mu_0 \dots \mu_n$ are model coefficients estimated by the MLE.

Table I shows the independent variables and variable coding used in W/CDM, and it includes one binary variable and three tri-class variables. TTC and TD which are two continuous variables are calculated in real time based on the traffic states.

IV. MODIFIED SOCIAL FORCE MODEL FOR PEDESTRIAN PATH PREDICTION

The classical social force model (SFM) was initially introduced by Helbing and Molnar (1995) which was used for the micro simulation of pedestrian kinetics. This model describes the conditions of pedestrians, and includes three basic forces: pedestrian driving force, interaction force from pedestrians, and repulsive force from obstacles [25].

On the basis of the basic SFM, Helbing *et al.* [26] also explored the interactions between pedestrians and vehicles in crosswalk. In this paper, modified social force model used for pedestrian path prediction includes four sources of social force: driving force from destination (\vec{F}_d), repulsive force from conflicting pedestrians (\vec{F}_p), attractive or repulsive force from crosswalk boundary (\vec{F}_b) and accelerating or repulsive

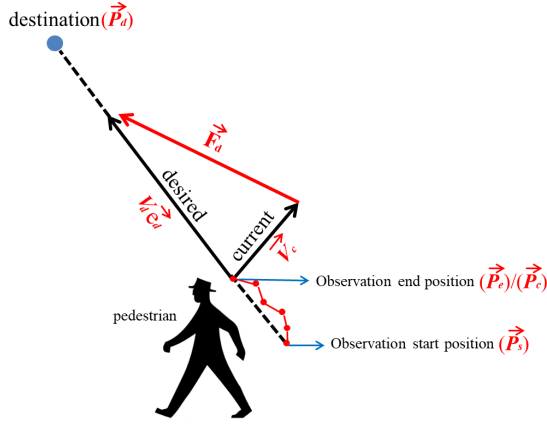


Fig. 2. Pedestrian driving force from destination.

force from straight-going vehicles (\vec{F}_v), and the resultant force ($\vec{F}_r(t_k)$) can be represented as:

$$\vec{F}_r(t_k) = \vec{F}_d + \vec{F}_P + \vec{F}_b + \vec{F}_v \quad (3)$$

The resultant speed vector $\vec{V}_r(t_k)$ can be written as:

$$\vec{V}_r(t_k) = \vec{V}_c(t_k) + \vec{F}_r(t_k) \Delta t \quad (4)$$

where $\vec{V}_c(t_k)$ is the current speed vector at the time step t_k ; Δt is the time step which is set as 0.2s for simulation in this paper.

Then the pedestrian path prediction of the next position is given as:

$$\vec{P}_r(t_{k+1}) = \vec{P}_c(t_k) + \vec{V}_c(t_k) \Delta t + \frac{1}{2} \vec{F}_r(t_k) \Delta t^2 \quad (5)$$

where $\vec{P}_c(t_k)$ represents the current position vector at the time step t_k ; $\vec{P}_r(t_{k+1})$ represents the next position vector at the time step t_{k+1} .

A. Pedestrian Driving Force

Pedestrian driving force manifests the motivation that the pedestrian walks towards the destination, which presents the subjective mentality of the pedestrian and influences the individual behavior. As shown in Fig. 2, it is assumed that the pedestrian moves with the individual desired speed V_d and the desired direction \vec{e}_d towards the destination. The unit vector \vec{e}_d for the desired moving direction is calculated by the pedestrian current position \vec{P}_c and the destination position \vec{P}_d . The driving force is assumed to drive the pedestrian to adjust the current speed vector \vec{V}_c to move in the desired direction vector \vec{e}_d at a desired speed V_d within a relaxation time τ . In this paper, the unit vector \vec{e}_o of the direction of destination for pedestrians make their way is calculated by the pedestrian observation start position \vec{P}_s and the pedestrian observation end position \vec{P}_e at a time horizon of 1s. As the pedestrian path is predicted at a time horizon of 2s, the destination position \vec{P}_d can be shown by equation (6), which is the path of pedestrian

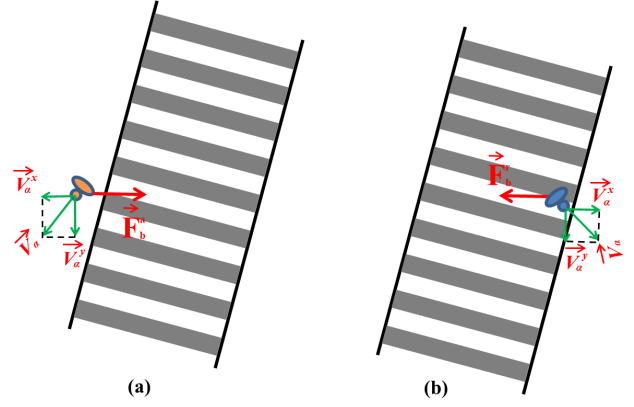


Fig. 3. Pedestrian force from crosswalk boundary: (a) attractive force and (b) repulsive force.

moving with the desired speed V_d after 3s.

$$\begin{cases} \vec{e}_o = \frac{\vec{P}_e - \vec{P}_s}{\|\vec{P}_e - \vec{P}_s\|} \\ \vec{P}_d = \vec{P}_c + 3V_d\vec{e}_o \end{cases} \quad (6)$$

The pedestrian driving force \vec{F}_d is shown below. In this paper, though the magnitude and direction of the unit vector \vec{e}_o in equation (6) are equal to those of the unit vectors \vec{e}_d in equation (8), the calculation methods of these two vectors are different. Here using different names and notations are for better understanding and distinguishing.

$$\vec{F}_d = \frac{(V_d\vec{e}_d - \vec{V}_c)}{\tau} \quad (7)$$

$$\vec{e}_d = \frac{\vec{P}_d - \vec{P}_c}{\|\vec{P}_d - \vec{P}_c\|} = \frac{3V_d\vec{e}_o}{\|3V_d\vec{e}_o\|} = \vec{e}_o \quad (8)$$

B. Pedestrian Force From Crosswalk Boundary

In general, when pedestrians enter into the crosswalk, they would like to walk inside the crosswalk boundary. It is assumed that pedestrian may walk out of the crosswalk boundary for collision avoidance with other pedestrians. However, almost everyone may move back into the crosswalk boundary gradually for security reasons. Then an attractive force \vec{F}_{ba}^a will be developed to draw them back into the crosswalk boundary which can be shown in Fig. 3(a). As shown in Fig. 3(b), when the pedestrian is inside the crosswalk whose velocity component is directed toward the crosswalk boundary, a repulsive force \vec{F}_{ba}^r will be developed to make the pedestrian keep a certain distance from the boundary.

The social force \vec{F}_b from crosswalk boundary is shown below:

$$\vec{F}_b = \begin{cases} \vec{F}_{ba}^a = A_b^a \exp\left(\frac{(r_a - d_a)}{B_b^a}\right) \vec{n}_{ab}, & \text{if pedestrian is} \\ & \text{outsidethe crosswalk boundary} \\ \vec{F}_{ba}^r = A_b^r \exp\left(\frac{-(r_a - d_a)}{B_b^r}\right) \vec{n}_{ba}, & \text{otherwise} \end{cases} \quad (9)$$

where A_b^a , B_b^a , A_b^r and B_b^r are the strength coefficients to be estimated; r_a is the radius of pedestrian a which is set as

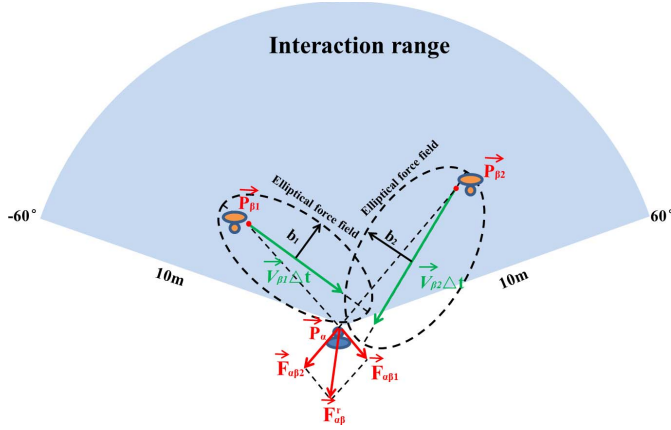


Fig. 4. Pedestrian repulsive force from conflicting pedestrians.

0.25m for simulation in this paper [27]; d_a is the distance between crosswalk boundary and pedestrian α ; \vec{n}_{ab} represents the normalized vector pointing from pedestrian α to crosswalk boundary and \vec{n}_{ba} represents the normalized vector pointing from crosswalk boundary to pedestrian α .

C. Pedestrian Repulsive Force From Conflicting Pedestrians

As shown in Fig. 4, it is supposed that each pedestrian within the interaction range will generate an elliptical force field which will result in repulsive force to the subject pedestrian. The angle of the interaction range is designed as 120° , and the radius of the interaction range is designed as 10m [19], [28], [29]. Different from the classical social force model, in this paper, the relative distance b_i which is the length of the semi-minor axis of the elliptical force field is considered as the distance between the centers of the pedestrians. Thus, the resultant force $\vec{F}_{\alpha\beta}^r$ from the conflicting pedestrians can be represented as:

$$\begin{cases} \vec{F}_{\alpha\beta}^r = \sum_{i=1}^n A_p \exp\left(\frac{(r_{ij} - b_i)}{B_p}\right) \vec{n}_{\beta_i\alpha} \\ b_i = \frac{1}{2} \sqrt{\left(\|\vec{P}_{\beta_i} - \vec{P}_\alpha\| + \|\vec{P}_{\beta_i} + \vec{V}_{\beta_i} \Delta t - \vec{P}_\alpha\|\right)^2 - \left(\|\vec{V}_{\beta_i} \Delta t\|\right)^2} \end{cases} \quad (10)$$

where A_p and B_p are the strength coefficients to be estimated; \vec{P}_α is the current position of pedestrian α ; \vec{P}_{β_i} is the current position of conflicting pedestrian β_i ; \vec{V}_{β_i} is the current velocity of conflicting pedestrian β_i ; $\vec{n}_{\beta_i\alpha}$ represents the normalized vector pointing from pedestrian β_i to pedestrian α ; r_{ij} is the sum of the pedestrians' radius; j represents one of the conflicting pedestrians to the subject pedestrian α and n is the number of the conflicting pedestrians.

D. Pedestrian Force From Straight-Going Vehicle

It is assumed that pedestrians are influenced by the approaching straight-going vehicle once the vehicle has entered into the personal interaction range. Fig. 5 shows the personal interaction range, similar to the interaction range with pedestrians, the angle of the interaction range is designed as 120° , and the radius of the interaction range is set as 35m [18]. As shown in Fig. 5, in this paper, the potential collision point

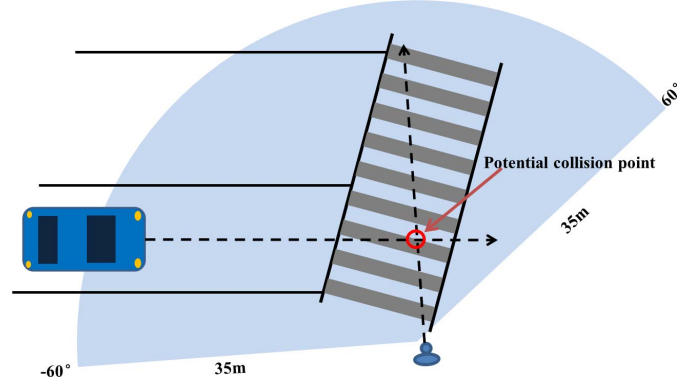


Fig. 5. Conflict with straight-going vehicle.

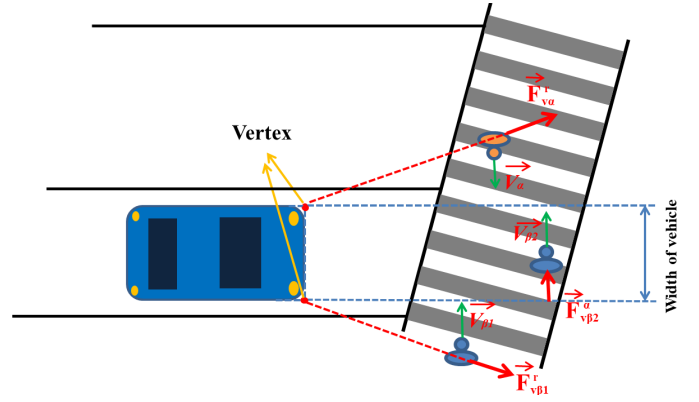


Fig. 6. Pedestrian force from straight-going vehicle.

is defined as the expected point for the approaching straight-going vehicle and pedestrian to conflict with each other if they keep their current directions. In other words, the potential collision point is just the intersection of the approaching straight-going vehicle and pedestrian future paths based on their directions.

As shown in Fig. 6, pedestrians will take steps to avoid collision with the straight-going vehicle, and this situation is similar to the collision avoidance with the conflicting pedestrians. It is supposed that pedestrian β_2 who enters into the crosswalk is in front of the approaching vehicle and is within the width of the vehicle, an accelerating force \vec{F}_{va}^a will be developed to make the pedestrian quickly get away from the potential collision point. When the pedestrian α or β_1 is on the left/right side of the approaching vehicle and is walking close to the vehicle in lateral direction, a repulsive force \vec{F}_{va}^r from each adjacent acme of the approaching vehicle can be generated. The repulsive force can make the pedestrian maintain a safe distance from the approaching vehicle. Thus, a composite force \vec{F}_v is developed to present the pedestrian force from the straight-going vehicle.

$$\vec{F}_v = \begin{cases} \vec{F}_{va}^a = A_v^a \exp\left(\frac{(r_{va} - d_{va})}{B_v^a}\right) \vec{e}_d, & \text{if pedestrian is} \\ & \text{in front and within the width of vehicle} \\ \vec{F}_{va}^r = A_v^r \exp\left(\frac{(r_{va} - d_{nva})}{B_v^r}\right) \vec{n}_{va}, & \text{if } \vec{V}_\alpha * \vec{n}_{va} < 0 \end{cases} \quad (11)$$

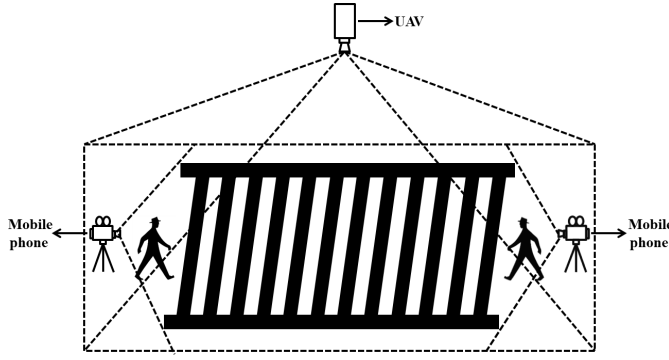


Fig. 7. Schematic diagram of the shooting scene.

where A_v^a , B_v^a , A_v^r and B_v^r are the strength coefficients to be estimated; $r_{v\alpha}$ is the sum of the vehicle's and pedestrian's radius; $d_{v\alpha}$ is the distance between the vehicle and pedestrian α ; \vec{e}_d represents the normalized vector of the desired direction of pedestrian α ; $d_{nv\alpha}$ represents the distance between the pedestrian α and the vertex that is the nearest point to the subject pedestrian and $\vec{n}_{v\alpha}$ represents the normalized vector pointing from the nearest vertex to the subject pedestrian α .

V. PARAMETER CALIBRATION OF MSFM AND W/CDM

A. Traffic Data Collection

In this paper, an unmanned aerial vehicle (UAV) with a visual camera was used for traffic data collection. The UAV can get a full picture of the pedestrian and vehicle scenes from a top-down view. The flight altitude was set approximately 60m with no interference to the traffic environment. In order to identify the gender and age of the crossing pedestrians, two mobile phones used for video recorded were placed on both sides of the crosswalk to collect the pedestrian data, and they were placed on fixed brackets which can be shown in Fig. 7. In this paper, the gender and age type of the crossing pedestrians were manually annotated from the video recorded by the mobile phones. In other words, the gender and age type of the crossing pedestrians were obtained by the tagging staff from the video recorded based on the human cognitive experience. Fig. 8 shows the scene of the traffic data collection from the UAV, which was an un-signalized crosswalk in Shanghai, China. The crosswalk is located at the Bo Le Road which is near a bus station and a supermarket. The length and width of the crosswalk are 19.8m and 6.2m. The traffic data was collected for five hours by the UAV and mobile phones. As the traffic environment is not controlled, all the traffic data collected is related to the real-life pedestrian and vehicle actions. Then the video recorded by the UAV was cut into 36000 images every 0.5s. The position coordinate points of pedestrians and straight-going vehicles were manually extracted from the images for analyzing the characteristics of the pedestrian crossing and calibrating the parameters of the models. The dataset includes the paths of 1509 pedestrians and 233 straight-going vehicles. All the pedestrians were made up of 478 young people (253 females and 225 males), 536 middle-aged people (251 females and

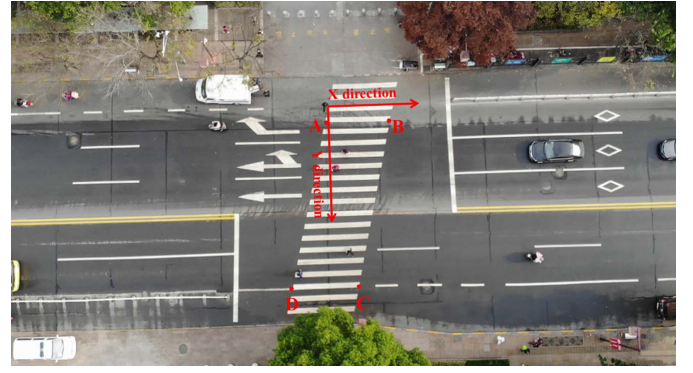


Fig. 8. Scene of the traffic data collection from the UAV.

285 males) and 495 old people (229 females and 266 males). In total, 48,200 position coordinate points (pedestrians and straight-going vehicles) were obtained from the video recorded every 0.5s, and 1200 suitable paths of pedestrians were made up of 48,200 position coordinate points.

As the dataset of the positions extracted from the images based on time series are just pixel values, the image point coordinates should be transformed into the real physical coordinates through the linear projective transformation, which is given by equation (12). In the linear projective transformation, four reference points (A, B, C, and D) are needed which are shown in Fig. 8. The real physical coordinates of the four points were obtained by the actual measurement. To take advantage of the linear projective transformation above, all the relevant variables of pedestrians and straight-going vehicles, such as positions, distances, velocities, accelerations and so on can be acquired either directly or by finite difference calculation.

$$\begin{cases} X_p + \frac{C_1 + C_2 X_i + C_3 Y_i}{1 + C_7 X_i + C_8 Y_i} = 0 \\ Y_p + \frac{C_4 + C_5 X_i + C_6 Y_i}{1 + C_7 X_i + C_8 Y_i} = 0 \end{cases} \quad (12)$$

where X_i , Y_i are the values of image point coordinates; X_p , Y_p are the values of physical coordinates; $C_1 \dots C_8$ are the parameters for the linear projective transformation.

B. Calibration Methodology

The calibration method used in this paper is based on the method adopted by Liu *et al.* [19]. There are many parameters in MSFM and W/CDM, some of the parameters can be measured from the observed data directly, and other non-measurable parameters need to be calibrated by the MLE. A three-stage process is adopted to calibrate the parameters [30], [31]:

- (1) The parameters such as interaction range, which are measurable data but difficult to be obtained from the real path data, are supported by referring to the relevant literature;
- (2) The parameters such as desired speed and relaxation time, which can be obtained from the real path data, are directly used.
- (3) The parameters such as strength coefficients, which have no specific physical meanings, are derived by the MLE.

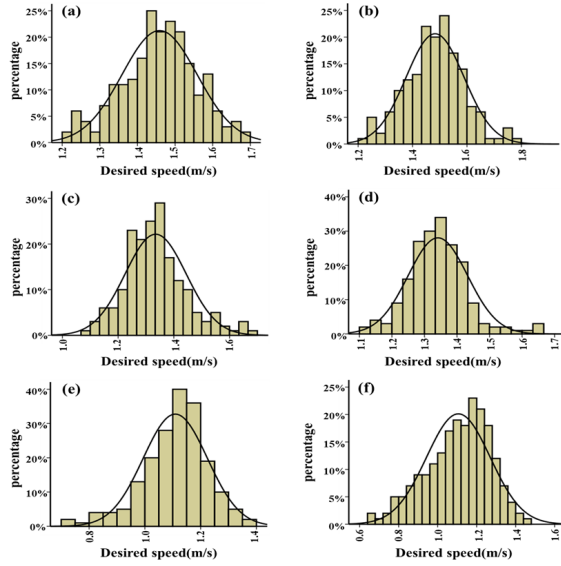


Fig. 9. Distribution of the desired speed by age and gender type: (a) young females, (b) young males, (c) middle-aged females, (d) middle-aged males, (e) old females and (f) old males.

C. Measurable Parameter Calibration

In this paper, there are four measurable parameters in MSFM, i.e. desired speed V_d by age and gender type, relaxation time τ by age and gender type, angle of interaction range and radius of interaction range for conflicting pedestrians and vehicles.

The interaction range is defined as the radius and angle at which a given standard object can be seen with naked eyes. Due to the conditional restrictions, it is difficult to directly identify the interaction range from the real path data. Thus, as described above, according to some related research results, for the conflicting pedestrian, the angle of the interaction range is designed as 120° , and the radius of the interaction range is designed as 10m [19], [28], [29], for the conflicting vehicle, the angle of the interaction range is designed as 120° , and the radius of the interaction range is designed as 35m [18].

Desired speed, by definition, is the individual average speed while a pedestrian crosses the crosswalk without any interference from the surrounding road users. The real path data was extracted when there were no conflicting pedestrians and straight-going vehicles, and also the crossing pedestrian should be inside the crosswalk boundary. The results for the desired speed of average value are showed in Fig. 9. It can be seen that the desired speed looks like following a normal distribution by age and gender type. It can be seen that the desired speed of young females is 1.45m/s and the standard deviation is 0.10m/s, the desired speed of young males is 1.48m/s and the standard deviation is 0.11m/s, the desired speed of middle-aged females is 1.32m/s and the standard deviation is 0.12m/s, the desired speed of middle-aged males is 1.34m/s and the standard deviation is 0.10m/s, the desired speed of old females is 1.12m/s and the standard deviation is 0.12m/s, the desired speed of old males is 1.10m/s and the standard deviation is 0.16m/s. The average desired speed of young males is the fastest, and old males is the lowest. As the

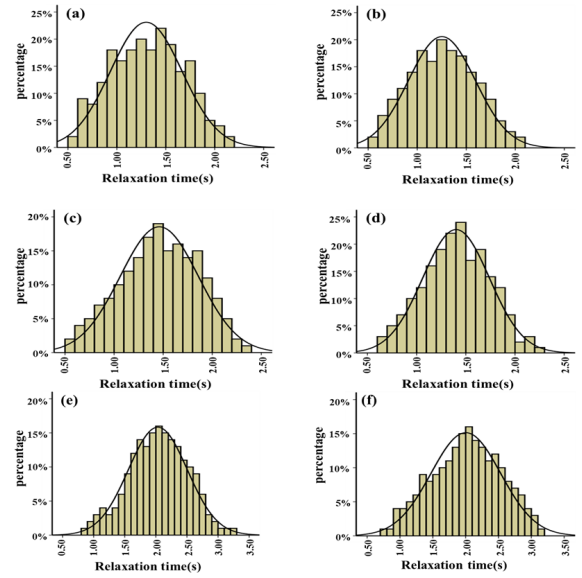


Fig. 10. Distribution of the relaxation time by age and gender type: (a) young females, (b) young males, (c) middle-aged females, (d) middle-aged males, (e) old females and (f) old males.

average desired speed of the same age type is close, in this paper, the desired speed of young type is specified as 1.45m/s, the desired speed of middle-aged type is specified as 1.32m/s, the desired speed of old type is specified as 1.10m/s.

Relaxation time, by definition, is the time for a pedestrian to accelerate from a lower current speed to the individual desired speed without any interference. To reduce the effects of other factors, the data used for relaxation time estimation is the same with the data used in desired speed estimation. Fig. 10 shows the distribution of the relaxation time by age and gender type which follows a normal distribution. It can be seen that the relaxation time of young females is 1.30s and the standard deviation is 0.37s, the relaxation time of young males is 1.25s and the standard deviation is 0.34s, the relaxation time of middle-aged females is 1.46s and the standard deviation is 0.40s, the relaxation time of middle-aged males is 1.40s and the standard deviation is 0.34s, the relaxation time of old females is 2.03s and the standard deviation is 0.47s, the relaxation time of old males is 2.00s and the standard deviation is 0.53s. The average relaxation time of old females is the longest, and young males is the shortest. In general, it is expected that the relaxation time of young type is much shorter than old type. As the average relaxation time of the same age type is close, in this paper, the relaxation time of young type is specified as 1.30s, the relaxation time of middle-aged type is specified as 1.46s, the relaxation time of old type is specified as 2.03s.

D. Non-Measurable Parameter Calibration

MLE is used to calibrate the non-measurable parameters of MSFM and W/CDM. As MSFM is a two-dimensional model (x and y direction), a two-dimensional MLE is used to calibrate the parameters [19], [32], [33]. The random error of equation (3) is supposed to have a bivariate normal probabilistic density function with a zero mean and a

TABLE II
CALIBRATION RESULTS OF MSFM

Parameters	Estimates	p-value	Description
A_b^a	0.6	0.01	Strength coefficients for attractive force from crosswalk boundary.
B_b^a	2.4	0.02	
A_b^r	1.5	0.02	Strength coefficients for repulsive force from crosswalk boundary.
B_b^r	3.3	0.03	
A_p	0.5	0.01	Strength coefficients for repulsive force from conflicting pedestrians.
B_p	2.0	0.03	
A_v^a	4.2	0.02	Strength coefficients for accelerating force from conflicting vehicle.
B_v^a	1.6	0.01	
A_v^r	2.8	0.02	Strength coefficients for repulsive force from conflicting vehicle.
B_v^r	2.2	0.02	

variance-covariance matrix (Σ). The likelihood L_k of each time step is linked directly to the probability density function of the normal distribution which is shown below:

$$L_k(\theta_r) = \frac{1}{2\pi |\Sigma|^{1/2}} e^{-\frac{(\tilde{F}_r(t_k) - \tilde{a}(t_k))^T \Sigma^{-1} (\tilde{F}_r(t_k) - \tilde{a}(t_k))}{2}} \quad (13)$$

$$\theta_r = [A_b^a, B_b^a, A_b^r, B_b^r, A_p, B_p, A_v^a, B_v^a, A_v^r, B_v^r] \quad (14)$$

where $\tilde{a}(t_k)$ is the observed acceleration at the time t_k ; θ_r is the summary of the parameters of MSFM which is to be estimated.

For a group of N independent pedestrians and the time steps of each pedestrian is M_i , the combination equation of the two-dimensional normal likelihood function can be presented as equation (15), as shown at the bottom of the next page. In order to simplify the solution calculation, a log-likelihood function which is obtained through the mathematical processing is presented as equation (16), as shown at the bottom of the next page. The maximum log-likelihood estimates of model non-measurable parameters for MSFM are achieved when equation (16) is maximized. It can be obtained by minimizing the negative log-likelihood, i.e., $-\ln L(\theta_r)$, in Matlab program. A 'fminunc' function in Matlab is used to find a minimum of the negative log-likelihood function with the model non-measurable parameters.

In this paper, 1200 suitable paths were annotated from the video recorded, 1000 paths were used to calibrate the parameters and 200 paths (annotated every 0.2s) were used to test the model accuracy. The parameter calibration result of MSFM is presented in Table II. The interrelated p-values of less than 0.05 indicate that all the parameters in MSFM are statistically significant. It can be seen that type coefficient A_v^a for the interaction strength of vehicle accelerating force has the largest value. This finding implies that a higher sensitivity of collision avoidance is formed from the conflicting vehicle on pedestrian crossing path.

Table III shows the result of the parameter calibration for W/CDMO. As the parameter sign for TTC has the maximum positive value, the result indicates that the probability of pedestrian crossing the crosswalk increases with TTC. As the parameter sign for vehicle type has the minimum negative value, the probability of pedestrian crossing the crosswalk

TABLE III
CALIBRATION RESULTS OF W/CDMO

Parameters	Estimates	p-value	Description
λ_0	-12.943	0.00	constant
λ_1	0.682	0.04	age type
λ_2	-0.886	0.03	gender type
λ_3	0.741	0.04	group size
λ_4	4.306	0.00	time to collision
λ_5	-2.267	0.02	vehicle type

TABLE IV
CALIBRATION RESULTS OF W/CDMI

Parameters	Estimates	p-value	Description
μ_0	-0.973	0.01	constant
μ_1	0.517	0.02	age type
μ_2	-0.091	0.02	gender type
μ_3	0.732	0.04	group size
μ_4	2.681	0.00	time difference
μ_5	-0.521	0.03	vehicle type

decreases with vehicle type, in other words, the larger the conflicting vehicle, the lower the probability that pedestrian will cross the crosswalk.

Table IV shows the result of the parameter calibration for W/CDMI. It can be seen that TD has a positive effect on pedestrian crossing behavior. Pedestrians tend to cross if the arrival time to the potential collision point is earlier than that of the conflicting vehicle. Vehicle type has a negative impact on pedestrian crossing behavior which is the same as that in W/CDMO.

VI. MODELS VALIDATION WITH OBSERVED DATA

In this section, the performance of the proposed W/CDM-MSFM based on the observed data is validated. The comparison of the predicted and observed results of W/CDMO and W/CDMI are demonstrated in Table V and Table VI, respectively. As shown in Table V, the average of the total percentage accuracy is higher than 93%, the true positive rate of the waiting decision is 97.3%, and the true positive rate of the crossing decision is 93.1%. Table VI shows that the proposed W/CDMI achieves more than 92% accuracy

TABLE V

COMPARISON OF THE PREDICTED AND OBSERVED RESULTS OF W/CDMO

Item	Predicted data	Accuracy
(True / False) positive	73/2	97.3%
(True / False) negative	27/2	93.1%

True/False positive = True/False waiting

True/False negative = True/False crossing

TABLE VI

COMPARISON OF THE PREDICTED AND OBSERVED RESULTS OF W/CDMI

Item	Predicted data	Accuracy
(True / False) positive	52/3	94.5%
(True / False) negative	72/6	92.3%

True/False positive = True/False waiting

True/False negative = True/False crossing

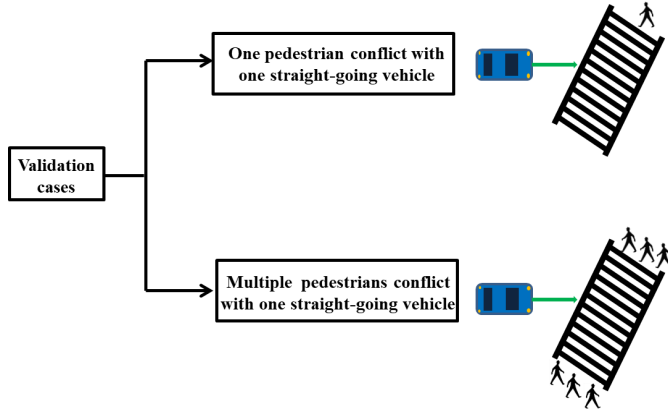


Fig. 11. Two typical cases for validation of MSFM.

to recognize pedestrians' waiting/crossing intentions, the true positive rate of the waiting decision is 94.5%, and the true positive rate of the crossing decision is 92.3%. The results of Table V and Table VI indicate that the proposed W/CDM has a high accuracy for predicting pedestrians' waiting/crossing intentions and is an acceptable model for pedestrian path prediction process.

After using W/CDM to judge pedestrians' waiting/crossing intentions when a straight-going vehicle is approaching, as shown in Fig. 11, two typical cases are selected to validate the accuracy of MSFM at a time horizon of 2s. The partial observation dataset of the pedestrians' paths is

separated into two groups according to the two typical cases, i.e., one pedestrian's path with one conflicting straight-going vehicle and multiple pedestrians' paths with one conflicting straight-going vehicle. In addition, to facilitate the comparison of the predicted results, two evaluation metrics are used to calculate the error of the predicted paths [18], [34], [35]:

(1) Average Final Displacement Error (FDE): this metric calculates the mean square error between the final observed paths and the final predicted paths of all pedestrians.

(2) Average Mean Absolute Percentage Error (MAPE): this metric calculates the mean percentage error between the final observed paths and the final predicted paths of all pedestrians.

$$FDE = \frac{\sum_{i=1}^N \|\vec{P}_r - \vec{P}_o\|_2}{N} \quad (17)$$

$$MAPE = \text{abs} \left(\frac{\sum_{i=1}^N (\|\vec{P}_r - \vec{P}_{o-1}\|_2 - \|\vec{P}_o - \vec{P}_{o-1}\|_2)}{N * \|\vec{P}_o - \vec{P}_{o-1}\|_2} \right) \quad (18)$$

where \vec{P}_r represents the final predicted path; \vec{P}_o represents the final observed path; \vec{P}_{o-1} represents the observed path 1s ago; N is the number of the pedestrians.

1) *Case I*: one pedestrian conflict with one conflicting straight-going vehicle

As shown in Fig. 12(a), the pedestrian enters into the crosswalk when one subject straight-going vehicle is approaching, and W/CDM-MSFM is used to predict the crossing path of the pedestrian for the next 2s. It is illustrated that the repulsive force from the straight-going vehicle has a significant effect on the pedestrian in this case. Fig. 12(b) shows the predicted results of the step-wise pedestrian path for 2s with the observed data and Fig. 12(c) shows the step-wise error between the predicted path and the observed path. The FDE for the moving path is 7.5cm and the MAPE for the moving path is 5.44%. It is found that the error of the predicted path is relatively small, in other words, the predicted results are in good agreement with the observed data.

2) *Case II*: multiple pedestrians conflict with one conflicting straight-going vehicle

As shown in Fig. 13(a), multiple pedestrians conflict with one straight-going vehicle, and determine to cross which using W/CDM to judge. It is demonstrated that the repulsive forces from the conflicting pedestrians and the composite forces from the straight-going vehicle have a significant impact in this case. The comparison of the predicting step-wise pedestrian path and the observed data for 2s is shown in Fig. 13(b), and the

$$L(\theta_r) = \prod_{i=1}^N \prod_{k=1}^M \frac{1}{2\pi |\sum|^{1/2}} e^{-\frac{(\vec{F}_r(t_k) - \vec{a}(t_k))^T \sum^{-1} (\vec{F}_r(t_k) - \vec{a}(t_k))}{2}}$$

$$= \frac{1}{(2\pi)^{M_1 M_2 \dots M_N}} \frac{1}{|\sum|^{M_1 M_2 \dots M_N / 2}} e^{-\frac{\sum_{i=1}^N \sum_{k=1}^{M_i} (\vec{F}_r(t_k) - \vec{a}(t_k))^T \sum^{-1} (\vec{F}_r(t_k) - \vec{a}(t_k))}{2}} \quad (15)$$

$$\ln L(\theta_r) = -M_1 M_2 \dots M_N \ln(2\pi) - \frac{M_1 M_2 \dots M_N}{2} \ln(|\sum|) - \frac{1}{2} \sum_{i=1}^N \sum_{k=1}^{M_i} (\vec{F}_r(t_k) - \vec{a}(t_k))^T \sum^{-1} (\vec{F}_r(t_k) - \vec{a}(t_k)) \quad (16)$$

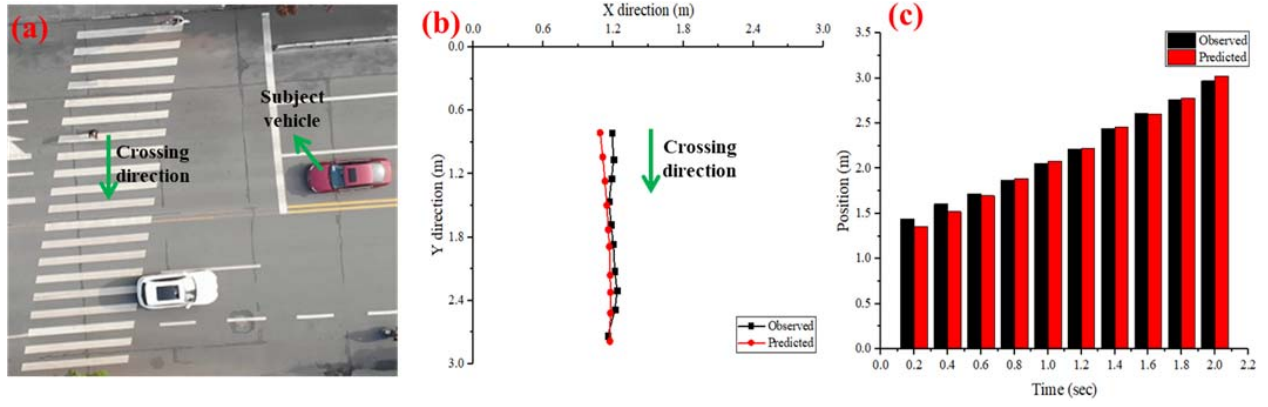


Fig. 12. One pedestrian conflict with one straight-going vehicle.

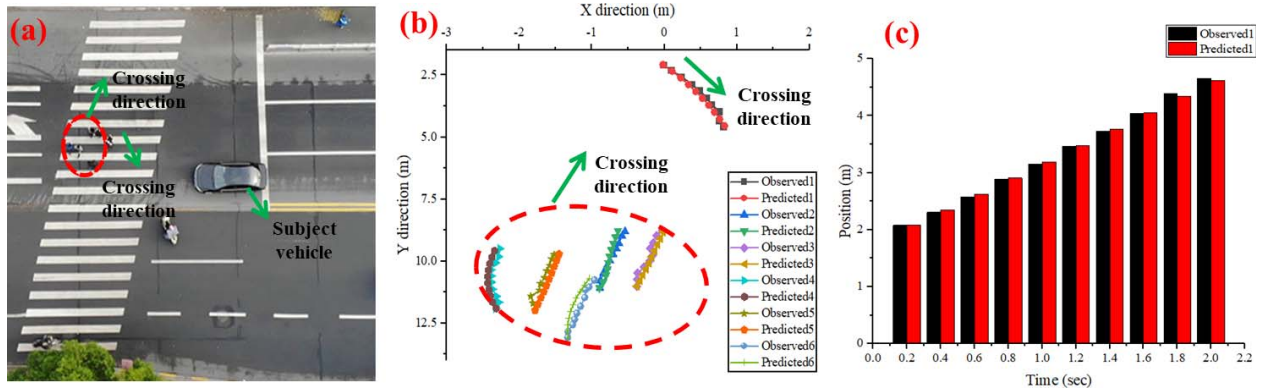


Fig. 13. Multiple pedestrians conflict with one straight-going vehicle.

step-wise error of one of the multiple pedestrians is shown in Fig. 13(c). The FDE for the moving path is 12.3cm and the MAPE for the moving path is 8.09%. The results illustrate that MSFM for pedestrian path prediction of multiple pedestrians' conflict with one straight-going vehicle is adequate as the error between the predicted and observed values is small. Therefore, the proposed MSFM can be used to predict the pedestrian path with acceptable accuracy.

In order to verify the performance of the proposed method (W/CDM-MSFM), a comparative test is conducted between the proposed method and five existing methods (i.e., EKF CV [7], EKF CA [12], LSTM [16], RNN [9], SFM [19]) in each case. As shown in Table VII, 100 groups of the average FDE and MAPE of each case for the predicted paths based on 6 methods at a time horizon of 2s are given. It can be seen that the proposed method has achieved outperform results with the lowest error of the average FDE and MAPE. The proposed W/CDM-MSFM takes the collision avoidance with pedestrians and vehicles, the reaction to crosswalk boundary based on sociology and social psychology into consideration. Particularly, the influence of pedestrian heterogeneous characteristics is also taken into account in W/CDM-MSFM, thereby leading to higher prediction accuracy than other existing methods. As the fair agreement among the predicted and observed paths is observed based on W/CDM-MSFM in Table VII, this indicates that the integrated method (W/CDM-MSFM) is an effective method, which gives us the confidence to use the

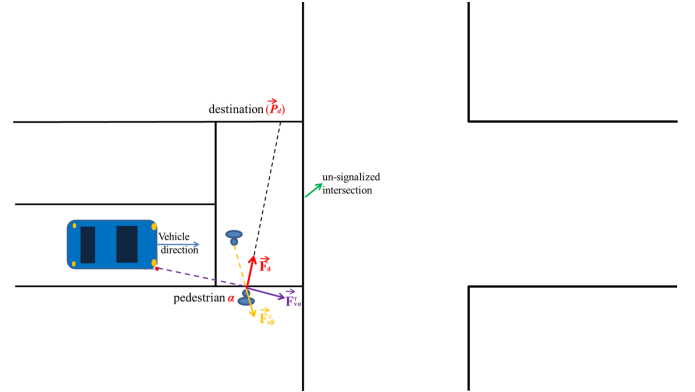


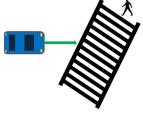
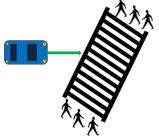
Fig. 14. Pedestrian social forces from destination, conflicting pedestrian and straight-going vehicle at un-signalized and unmarked intersection.

current method to predict the pedestrian path for autonomous driving with significant accuracy.

3) *Discussion:* the proposed method being used at un-signalized and unmarked intersections

The scene of un-signalized and unmarked intersections for pedestrian path prediction should also be focused on, where there is no clear priority for pedestrians and vehicles. The proposed model (W/CDM-MSFM) can be used for un-signalized and unmarked intersections. As shown in Fig.14, it is supposed that pedestrian α enters into the un-signalized and unmarked intersection, pedestrian social forces from destination (\vec{F}_d),

TABLE VII
FDE AND MAPE OF THE PREDICTED PATHS BASED ON 6 METHODS

Case classification	Groups of pedestrians	Methods	FDE (cm)	MAPE
Case I 	100	EKF CV ^[7]	29.1	17.3%
		EKF CA ^[12]	34.8	22.9%
		LSTM ^[16]	18.2	12.8%
		RNN ^[9]	22.0	15.2%
		SFM ^[19]	19.6	14.5%
		WCDM-MSFM	13.6	8.7%
Case II 	100	EKF CV ^[7]	34.7	19.6%
		EKF CA ^[12]	42.6	28.4%
		LSTM ^[16]	21.1	13.7%
		RNN ^[9]	23.6	14.9%
		SFM ^[19]	25.2	18.3%
		WCDM-MSFM	16.2	9.6%

conflicting pedestrian ($\vec{F}_{\alpha\beta}^r$) and straight-going vehicle (\vec{F}_{va}^r) can be developed. This scene is similar to the scene of un-signalized crosswalks for pedestrian path prediction, except that the force from the crosswalk boundary is removed. In other words, the proposed method is suitable for both un-signalized crosswalks and un-signalized and unmarked intersections, and pedestrians may become more cautious when crossing the un-signalized and unmarked intersections based on the sociology and social psychology. At the same time, the new video used for traffic data collection at un-signalized and unmarked intersections need to be recorded, and the parameters used in W/CDM-MSFM for un-signalized and unmarked intersections should be recalibrated by the MLE. In a word, with the help of the pedestrian path prediction method (W/CDM-MSFM), pedestrian safety is protected and traffic efficiency is improved for autonomous driving at un-signalized and unmarked intersections.

VII. CONCLUSION

In this paper, pedestrian path prediction for autonomous driving at an un-signalized crosswalk is systematically studied using W/CDM-MSFM within pedestrian heterogeneous characteristics consideration. The non-measurable parameters of the developed models are calibrated by the MLE. Finally, the models are validated with the existing methods based on the observed data. The following conclusions can be drawn from the investigation within the limitations and considerations in this study:

1. Two waiting/crossing decision models (W/CDM) with surrounding traffic states and pedestrian heterogeneous characteristics (age and gender) are developed. The models are intended to predict the pedestrian's real waiting/crossing intention when a vehicle is approaching and the predicted results are in good agreement with the observed data.
2. Heterogeneous pedestrian characteristics for age and gender type are taken into account in the humanoid microscopic dynamic MSFM for the first time, and the collision avoidance with pedestrians and straight-going vehicles, and the reaction to crosswalk boundary based on sociology and social psychology are also taken into

account for improving pedestrian path prediction accuracy. In addition, the desired speed and relaxation time for age and gender type are different, the average desired speed of young type is the fastest, and the average relaxation time of the old type is the longest.

3. Different from the repulsive force from the conflicting pedestrians, a novel composite force is developed to present the pedestrian force from the conflicting straight-going vehicle.
4. The calibration of the non-measurable parameters for the developed models is described, and the parameters are statistically significant with the interrelated p-values which are less than 0.05.
5. Comparing with the existing methods, the integrated W/CDM-MSFM method is excellent for predicting the pedestrian path of 2s at an un-signalized crosswalk with a fair degree of precision, which is of great significance in autonomous driving domain for protecting pedestrian safety and improving traffic efficiency with acceptable accuracy.

However, there are still several problems needing solving in future work. For example, the reaction of pedestrians to electric bicycle and the reaction of electric bicycle to vehicle should be future considered. In addition, the proposed W/CDM-MSFM method should also be actually tested in our autonomous vehicle for pedestrian path prediction with the help of a variety of sensors, such as radar, cameras and LIDAR. These problems will be improved in our future work.

AUTHOR CONTRIBUTIONS

Conceptualization: Xi Zhang and Hao Chen.
Data curation: Hao Chen and Wenqiang Jin.
Formal analysis: Xi Zhang and Hao Chen.
Funding acquisition: Xi Zhang.
Investigation: Xi Zhang and Hao Chen.
Methodology: Xi Zhang and Hao Chen.
Project administration: Xi Zhang.
Resources: Xi Zhang and Hao Chen.
Software: Hao Chen.
Supervision: Wenyan Yang.
Validation: Hao Chen.

Visualization: Hao Chen, Wenyan Yang, Wenqiang Jin and Wangwang Zhu.

**Writing-original
draft:** Hao Chen.

Writing-review

& editing: Xi Zhang and Hao Chen.

REFERENCES

- [1] L. Zheng, K. Ismail, and X. Meng, "Investigating the heterogeneity of postencroachment time thresholds determined by peak over threshold approach," *Transp. Res. Record, J. Transp. Res. Board*, vol. 2601, no. 1, pp. 17–23, Jan. 2016.
- [2] J. F. P. Kooij, N. Schneider, F. Flohr, and D. M. Gavrila, "Context-based pedestrian path prediction," in *Proc. Euro. Conf. Comput. Vis.*, Cham, Switzerland: Springer, 2014, pp. 618–633.
- [3] R. Quintero, J. Almeida, D. F. Llorca, and M. A. Sotelo, "Pedestrian path prediction using body language traits," in *Proc. IEEE Intell. Vehicles Symp. Proc.*, Jun. 2014, pp. 317–323.
- [4] M. M. Meinecke *et al.*, "Strategies in terms of vulnerable road user protection," EU Project, Eur. Commission DG INFSO, Brussels, Belgium, Tech. Rep. SAVE-U(IST-2001-34040), Deliverable D6, 2003.
- [5] E. Sacchi, T. Sayed, and P. DeLeur, "A comparison of collision-based and conflict-based safety evaluations: The case of right-turn smart channels," *Accid. Anal. Prev.*, vol. 59, pp. 260–266, Jun. 2013.
- [6] P. Songchitruksa and A. P. Tarko, "The extreme value theory approach to safety estimation," *Accident Anal. Prevention*, vol. 38, no. 4, pp. 811–822, Jul. 2006.
- [7] C. G. Keller, C. Hermes, and D. M. Gavrila, "Will the pedestrian cross? Probabilistic path prediction based on learned motion features," in *Pattern Recognition (Lecture Notes in Computer Science)*, vol. 6835, R. Mester and M. Felsberg, Eds. Berlin, Germany: Springer, Aug. 2011, pp. 386–395.
- [8] G. Habibi, N. Jaipuria, and J. P. How, "Context-aware pedestrian motion prediction in urban intersections," 2018, *arXiv:1806.09453*. [Online]. Available: <http://arxiv.org/abs/1806.09453>
- [9] C. Song *et al.*, "Human trajectory prediction for automatic guided vehicle with recurrent neural network," *J. Eng.*, vol. 2018, no. 16, pp. 1574–1578, Nov. 2018.
- [10] Y. Zheng, T. Chase, L. Eleftheriadou, B. Schroeder, and V. P. Sisiopiku, "Modeling vehicle–pedestrian interactions outside of crosswalks," *Simul. Model. Pract. Theory*, vol. 59, pp. 89–101, Dec. 2015.
- [11] D. Zhang, H. Zhu, L. Du, and S. Hostikka, "An optimization-based overtaking model for unidirectional pedestrian flow," *Phys. Lett. A*, vol. 382, no. 44, pp. 3172–3180, Nov. 2018.
- [12] N. Schneider and D. M. Gavrila, "Pedestrian path prediction with recursive Bayesian filters: A comparative study," *Pattern. Recognit.*, vol. 8142, pp. 174–183, Sep. 2013.
- [13] R. Q. Minguez, I. P. Alonso, D. Fernandez-Llorca, and M. A. Sotelo, "Pedestrian path, pose, and intention prediction through Gaussian process dynamical models and pedestrian activity recognition," *IEEE Trans. Intell. Transp. Syst.*, vol. 20, no. 5, pp. 1803–1814, May 2019.
- [14] Y. Li, M. L. Mekhalif, M. M. Al Rahhal, E. Othman, and H. Dhahri, "Encoding motion cues for pedestrian path prediction in dense crowd scenarios," *IEEE Access*, vol. 5, pp. 24368–24375, 2017.
- [15] C. G. Keller and D. M. Gavrila, "Will the pedestrian cross?: A study on pedestrian path prediction," *IEEE Trans. Intell. Transp. Syst.*, vol. 15, no. 2, pp. 494–506, Apr. 2014.
- [16] K. Saleh, M. Hossny, and S. Nahavandi, "Intent prediction of pedestrians via motion trajectories using stacked recurrent neural networks," *IEEE Trans. Intell. Vehicles*, vol. 3, no. 4, pp. 414–424, Dec. 2018.
- [17] S. Yi, H. Li, and X. G. Wang, "Pedestrian behavior understanding and prediction with deep neural networks," in *Computer Vision—ECCV*, vol. 9905, B. Leibe, J. Matas, N. Sebe, and M. Welling, Eds. Amsterdam, The Netherlands: Springer, Sep. 2016, pp. 263–279.
- [18] W. Zeng, P. Chen, G. Yu, and Y. Wang, "Specification and calibration of a microscopic model for pedestrian dynamic simulation at signalized intersections: A hybrid approach," *Transp. Res. C, Emerg. Technol.*, vol. 80, pp. 37–70, Jul. 2017.
- [19] M. Liu, W. Zeng, P. Chen, and X. Wu, "A microscopic simulation model for pedestrian-pedestrian and pedestrian-vehicle interactions at crosswalks," *PLoS ONE*, vol. 12, no. 7, Art. no. e0180992.
- [20] C. Ningbo, W. Wei, Q. Zhaowei, Z. Liying, and B. Qiaowen, "Simulation of pedestrian crossing behaviors at unmarked roadways based on social force model," *Discrete Dyn. Nature Soc.*, vol. 2017, pp. 1–15, Sep. 2017.
- [21] B. Anvari, M. G. H. Bell, A. Sivakumar, and W. Y. Ochieng, "Modelling shared space users via rule-based social force model," *Transp. Res. C, Emerg. Technol.*, vol. 51, pp. 83–103, Feb. 2015.
- [22] N. Rinke, C. Schiermeyer, F. Pascucci, V. Berkahn, and B. Friedrich, "A multi-layer social force approach to model interactions in shared spaces using collision prediction," *Transp. Res. Procedia*, vol. 25, pp. 1249–1267, May 2017.
- [23] L. Huang, J. Wu, F. You, Z. Lv, and H. Song, "Cyclist social force model at unsignalized intersections with heterogeneous traffic," *IEEE Trans. Ind. Informat.*, vol. 13, no. 2, pp. 782–792, Apr. 2017.
- [24] S. Marisamynathan and P. Vedagiri, "Modeling pedestrian delay at signalized intersection crosswalks under mixed traffic condition," *Procedia - Social Behav. Sci.*, vol. 104, pp. 708–717, Dec. 2013.
- [25] D. Helbing and P. Molnár, "Social force model for pedestrian dynamics," *Phys. Rev. E, Stat. Phys. Plasmas Fluids Relat. Interdiscip. Top.*, vol. 51, no. 5, pp. 4282–4286, May 1995.
- [26] D. Helbing, I. J. Farkas, P. Molnar, and T. Vicsek, "Simulation of pedestrian crowds in normal and evacuation situations," *Pedestrian Evacuation Dyn.*, vol. 21, no. 2, pp. 21–58, 2002.
- [27] *Human Dimensions of Chinese Adults*, Standard GB 10000-88, Oct. 1988.
- [28] G. Antonini, M. Bierlaire, and M. Weber, "Discrete choice models of pedestrian walking behavior," *Transp. Res. B, Methodol.*, vol. 40, no. 8, pp. 667–687, Sep. 2006.
- [29] R.-Y. Guo, S. C. Wong, H.-J. Huang, P. Zhang, and W. H. K. Lam, "A microscopic pedestrian-simulation model and its application to intersecting flows," *Phys. A, Stat. Mech. Appl.*, vol. 389, no. 3, pp. 515–526, Feb. 2010.
- [30] W. Zeng, P. Chen, H. Nakamura, and M. Iryo-Asano, "Application of social force model to pedestrian behavior analysis at signalized crosswalk," *Transp. Res. C, Emerg. Technol.*, vol. 40, pp. 143–159, Mar. 2014.
- [31] Z.-W. Qu, N.-B. Cao, Y.-H. Chen, L.-Y. Zhao, Q.-W. Bai, and R.-Q. Luo, "Modeling electric bike–car mixed flow via social force model," *Adv. Mech. Eng.*, vol. 9, no. 9, Sep. 2017, Art. no. 168781401771964.
- [32] W. Daamen and S. Hoogendoorn, "Calibration of pedestrian simulation model for emergency doors by pedestrian type," *Transp. Res. Record, J. Transp. Res. Board*, vol. 2316, no. 1, pp. 69–75, Jan. 2012.
- [33] M. Ko, T. Kim, and K. Sohn, "Calibrating a social-force-based pedestrian walking model based on maximum likelihood estimation," *Transportation*, vol. 40, no. 1, pp. 91–107, Jan. 2013.
- [34] A. Alahi, K. Goel, V. Ramanathan, A. Robicquet, L. Fei-Fei, and S. Savarese, "Social LSTM: Human trajectory prediction in crowded spaces," in *Proc. IEEE Conf. Comput. Vis. Pattern Recognit. (CVPR)*, Jun. 2016, pp. 961–971.
- [35] H. Xue, D. Q. Huynh, and M. Reynolds, "SS-LSTM: A hierarchical LSTM model for pedestrian trajectory prediction," in *Proc. IEEE Winter Conf. Appl. Comput. Vis. (WACV)*, Mar. 2018, pp. 1186–1194.



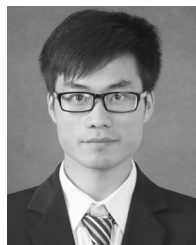
Xi Zhang (Senior Member, IEEE) received the B.Sc. degree in applied mathematics, the B.E. degree in information and control engineering, and the M.E. and Ph.D. degrees in power electronics and electric power drive from Shanghai Jiao Tong University (SJTU), Shanghai, China, in 2002, 2004, and 2007, respectively.

From September 2007 to July 2009, he held a post-doctoral position at the Department of Electrical and Computer Engineering, University of Michigan–Dearborn, Dearborn, MI, USA. He is currently a Full Professor with the Institute of Intelligent and Connected Automobile and National Engineering Laboratory for Automotive Electronics and Control Technology, SJTU. His research interests include intelligent and connected automobile, intelligent transportation, power management strategies, power electronics devices, and electric motor control systems for alternative-fuel vehicles.



Hao Chen received the M.S. degree in mechanical engineering and automation from Jiangsu University, Zhenjiang, China, in 2011. He is currently pursuing the Ph.D. degree in mechanical engineering with the School of Mechanical Engineering, Shanghai Jiao Tong University, Shanghai, China.

His research interests include the pedestrian path prediction for intelligent vehicles, pedestrian modeling and simulation, local path planning, and intelligent decision technology.



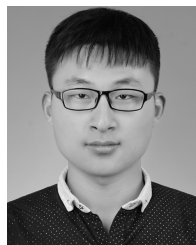
Wenqiang Jin received the B.S. degree in mechanical engineering from Shanghai Jiao Tong University, Shanghai, China, in 2017, where he is currently pursuing the M.S. degree in vehicle engineering.

He is also a Visiting Student with the Argonne National Laboratory, Lemont, IL, USA, since July 2018. His research interests include the intelligent transportation systems, adaptive traffic signal control, traffic modeling and simulation, and connected vehicle technology.



Wenyan Yang received the B.S. degree in mechanical engineering from Southeast University, Nanjing, China, in 2017. He is currently pursuing the M.S. degree in mechanical engineering with Shanghai Jiao Tong University, Shanghai, China.

His research interests include the pedestrian path prediction for intelligent vehicles, intelligent decision, and machine learning.



Wangwang Zhu received the M.S. degree in vehicle engineering from Shanghai Jiao Tong University, Shanghai, China, in 2019, where he is currently pursuing the Ph.D. degree in mechanical engineering with the School of Mechanical Engineering.

His research interests include decision making, local path planning, and execution and control algorithms for autonomous driving vehicles.